Eur. Phys. J. A **7**, 421–427 (2000)

THE EUROPEAN PHYSICAL JOURNAL A

Phenomenology of the deuteron electromagnetic form factors

The Jefferson Lab t_{20} Collaboration
D. Abbott[6], A. Ahmidouch[5,9], H. Anklin[8], J. Arvieux[10,12], J. Ball[1,10], S. Beedoe[9], E.J. Beise[4], L. Bimbot[12], W. Boeglin[8], H. Breuer[4], R. Carlini[6], N.S. Chant[4], S. Danagoulian[6,9], K. Dow[5], J.-E. Ducret[1], J. Dunne[6], L. Ewell[4], L. Eyraud[2], C. Furget[2], M. Garçon[1], R. Gilman[6,7], C. Glashausser[7], P. Gueye[6], K. Gustafsson[4], K. Hafidi[1], A. Honegger[3], J. Jourdan[3], S. Kox[2], G. Kumbartzki[7], L. Lu[2], A. Lung[4], P. Markowitz[8], J. McIntyre[7], D. Meekins[6], F. Merchez[2], J. Mitchell[6], R. Mohring[4], S. Mtingwa[9], H. Mrktchyan[11], D. Pitz[1,4,6], L. Qin[6], R. Ransome[7], J.-S. Réal[2], P.G. Roos[4], P. Rutt[7], R. Sawafta[9], S. Stepanyan[11], R. Tieulent[2], E. Tomasi-Gustafsson[1,10], W. Turchinetz[5], K. Vansyoc[6,a], J. Volmer[6,b], E. Voutier[2], C. Williamson[5], S.A. Wood[6], C. Yan[6], J. Zhao[3], W. Zhao[5]

[1] DAPNIA/SPhN, CEA/Saclay, 91191 Gif-sur-Yvette, France
[2] ISN, IN2P3-UJF, 38026 Grenoble, France
[3] Department of Physics, University of Basel, Switzerland
[4] University of Maryland, College Park, MD 20742, USA
[5] M.I.T.-Bates Linear Accelerator, Middleton, MA 01949, USA
[6] Thomas Jefferson National Accelerator Facility, Newport News, VA 23606, USA
[7] Rutgers University, Piscataway, NJ 08855, USA
[8] Florida International University, Miami, FL 33199, USA
[9] North Carolina A. & T. State University, Greensboro, NC 27411, USA
[10] LNS-Saclay, 91191 Gif-sur-Yvette, France
[11] Yerevan Physics Institute, 375036 Yerevan, Armenia
[12] IPNO, IN2P3, BP 1, 91406 Orsay, France

Received: 28 January 2000 / Revised version: 25 February 2000
Communicated by Th. Walcher

Abstract. A rigorous extraction of the deuteron charge form factors from tensor polarization data in elastic electron-deuteron scattering, at given values of the 4-momentum transfer, is presented. Then the world data for elastic electron-deuteron scattering is used to parameterize, in three different ways, the three electromagnetic form factors of the deuteron in the 4-momentum transfer range 0-7 fm^{-1}. This procedure is made possible with the advent of recent polarization measurements. The parameterizations allow a phenomenological characterization of the deuteron electromagnetic structure. They can be used to remove ambiguities in the form factors extraction from future polarization data.

PACS. 21.45.+v Few-body systems – 25.30.Bf Elastic electron scattering – 27.10.+h $A \leq 5$ – 13.40.Gp Electromagnetic form factors

1 Introduction

The deuteron, as the only two-nucleon bound state, has been the subject of many theoretical and experimental investigations. Since it has spin 1, its electromagnetic structure is described by three form factors, charge monopole G_C, charge quadrupole G_Q and magnetic dipole G_M, assuming P- and T-invariance. Measurements of elastic electron deuteron scattering observables provide quadratic combinations of these form factors. Since most of the data available come from differential cross section measurements, it has been customary, both in the data presentation and in the comparison with theoretical models, to use the two structure functions A and B defined hereafter, extracted from the cross section data by a Rosenbluth separation [1]. With the advent of tensor polarimeters and tensor polarized internal targets, polarization observables have been measured as well, which allow the separation of the two charge form factors.

The purpose of this work is twofold. First, in Sect. 2, the calculation of G_C and G_Q, at given values of the 4-momentum transfer Q, from polarization data together with (interpolated) A and B data is reexamined and updated with respect to previous work.

Then, in Sect. 3, parameterizations of the three deuteron form factors, in the 4-momentum transfer range $Q = 0 - 7$ fm^{-1}, are provided. Above 7 fm^{-1}, only small angle cross section data are available, preventing the sep-

[a] On leave from Old Dominion University, USA
[b] On leave from Vrije Universiteit, Amsterdam, The Netherlands

arate determination of the three form factors. We have determined the three deuteron electromagnetic form factors by fitting directly the measured differential cross section [2–20] and polarization [21–29] observables. This procedure eliminates the need for an intermediate determination of A and B, and results in a more realistic evaluation of errors for the form factors.

One parameterization is used for a determination of the node of the charge form factor G_C, while the application of the work of [30] allows the determination of reduced form factors in a helicity basis. The accuracy in the determination of these form factors is limited by the assumption of a one-photon exchange mechanism in the first order Born approximation at low Q, and by the accuracy of the data at intermediate to high momentum transfers. A third parameterization was recently applied for a precise determination of the rms–charge radius of the deuteron [31]. At low Q, Coulomb distortion was taken into account to extract precise values of G_C. Applying this correction resolved an old discrepancy between the deuteron radius determined via (e, e') and N–N scattering [32]. In the intermediate to high Q-range, other corrections such as the double scattering contribution to two photon exchange [33] should be considered, but they are at present neither accurately calculated nor experimentally determined.

2 Observables and form factors

2.1 e-d observables

Assuming single photon exchange, the electron-deuteron unpolarized elastic differential cross section can be written as

$$\begin{aligned}\frac{d\sigma}{d\Omega} &= \sigma_{NS}\cdot\left[G_C^2(Q^2)+\frac{8}{9}\eta^2 G_Q^2(Q^2)\right.\\ &\quad\left.+\frac{2}{3}\eta\varepsilon^{-1}(Q^2,\theta_e)G_M^2(Q^2)\right]\\ &\equiv \sigma_{NS}\cdot S,\end{aligned}\tag{1}$$

where σ_{NS} is the Mott differential cross section multiplied by the deuteron recoil factor, θ_e the electron scattering angle, $\eta = Q^2/4M_d^2$, M_d the deuteron mass; $\varepsilon = [1+2(1+\eta)\tan^2(\theta_e/2)]^{-1}$ is related to the virtual photon polarization. The quantity $S \equiv A + B\tan^2(\theta_e/2)$ defines the usual A and B elastic structure functions.

The tensor polarization observables t_{2q}, or equivalently the analyzing powers T_{2q}, have been measured as well. Their expression as a function of the three form factors, still in the one-photon exchange approximation, is given by:

$$-\sqrt{2}\cdot S\cdot t_{20} = \frac{8}{3}\eta G_C G_Q + \frac{8}{9}\eta^2 G_Q^2 + \frac{1}{3}\eta\varepsilon^{-1}G_M^2 \tag{2}$$

$$\sqrt{3}\cdot S\cdot t_{21} = 2\eta\left(\eta+\eta^2\sin^2\frac{\theta_e}{2}\right)^{1/2} G_M G_Q \sec\frac{\theta_e}{2} \tag{3}$$

$$-2\sqrt{3}\cdot S\cdot t_{22} = \eta G_M^2. \tag{4}$$

2.2 Calculation of G_C and G_Q

The charge form factors are here extracted from $t_{20}(Q,\theta_e)$ data, together with $A(Q)$ and $B(Q)$ (interpolated) data. The analyses presented in [22,26] need to be updated, because of new t_{20} [21,23,25] and A [2,4] data. In particular, the parameterization of A used in [26] gave a very small weight to the then only existing high Q data [5] and is lower than the new data [2,4] around 4.5 fm^{-1}. Furthermore, we present here a more compact solution and a more rigorous treatment of errors.

For our purpose, it is useful to define new quantities $A_0 \equiv A - B/2(1+\eta)$ and $\tilde{t}_{20}$ [26], derived respectively from A and t_{20} by eliminating the magnetic contribution:

$$\begin{aligned}\tilde{t}_{20} &\equiv -\frac{\frac{8}{3}\eta G_C G_Q + \frac{8}{9}\eta^2 G_Q^2}{\sqrt{2}\,(G_C^2+\frac{8}{9}\eta^2 G_Q^2)}\\ &= \frac{S\cdot t_{20} + B/4\sqrt{2}\varepsilon(1+\eta)}{A_0}\end{aligned}\tag{5}$$

Using the reduced form factors $g_C = G_C/\sqrt{A_0}$ and $g_Q = 2\eta G_Q/3\sqrt{A_0}$, (1,2,5) lead to:

$$g_C^2 + 2g_Q^2 = 1 \tag{6}$$

$$2g_C g_Q + g_Q^2 = p \equiv -\tilde{t}_{20}/\sqrt{2} \tag{7}$$

where p (or conventionnally p_{ZZ}) is the tensor polarization in Cartesian notation (also called alignment). There are four solutions to these equations given by

$$(g_Q^{\pm})^2 = \frac{2+p\pm\sqrt{\Delta}}{9} \tag{8}$$

with $\Delta = 8(1-p)(\frac{1}{2}+p)$ and $g_C^{\pm}$ from (7). The physical solution is easily selected at small Q from the static moments ($g_C(0)=1,\ g_Q(0)=0$). It corresponds to the choice of a minus sign in (8) and of $g_Q > 0$. Since $\tilde{t}_{20}$ and t_{21}, both proportional to G_Q, do not cross zero at a same value of Q [21,26], g_Q has to remain positive over the whole range considered in this work. The two remaining solutions (g_Q^+, g_C^+) and (g_Q^-, g_C^-) cross each other at values Q_{min} and Q_{max} where $\tilde{t}_{20}$ reaches its extrema $-\sqrt{2}$ and $+\sqrt{2}/2$ ($\Delta = 0$). The physical solution must switch from "$-$" to "$+$" at $Q = Q_{min}$ and then back to "$-$" at Q_{max} in order to ensure a continuity of the form factor derivatives. For polarization data close to these extrema, Q may be below or above the *a priori* unknown Q_{min} (or Q_{max}), and the choice of solution is ambiguous. Q_{min}, from our three global fits to the $e-d$ data (see Sect. 3), is determined to be close to 3.3 fm^{-1}. On the other hand, there are not enough polarization data to constrain the value of Q_{max}, so that the above mentioned ambiguity remains around $Q \simeq 6-8$ fm^{-1}. This is the case for the two points at highest Q in [21].

An additional complication arises for five polarization data points in [21–23,26,27] which lay partially outside the physical region $-\sqrt{2} \le \tilde{t}_{20} \le 1/\sqrt{2}$. This situation is quite probable for points with finite errors close to a

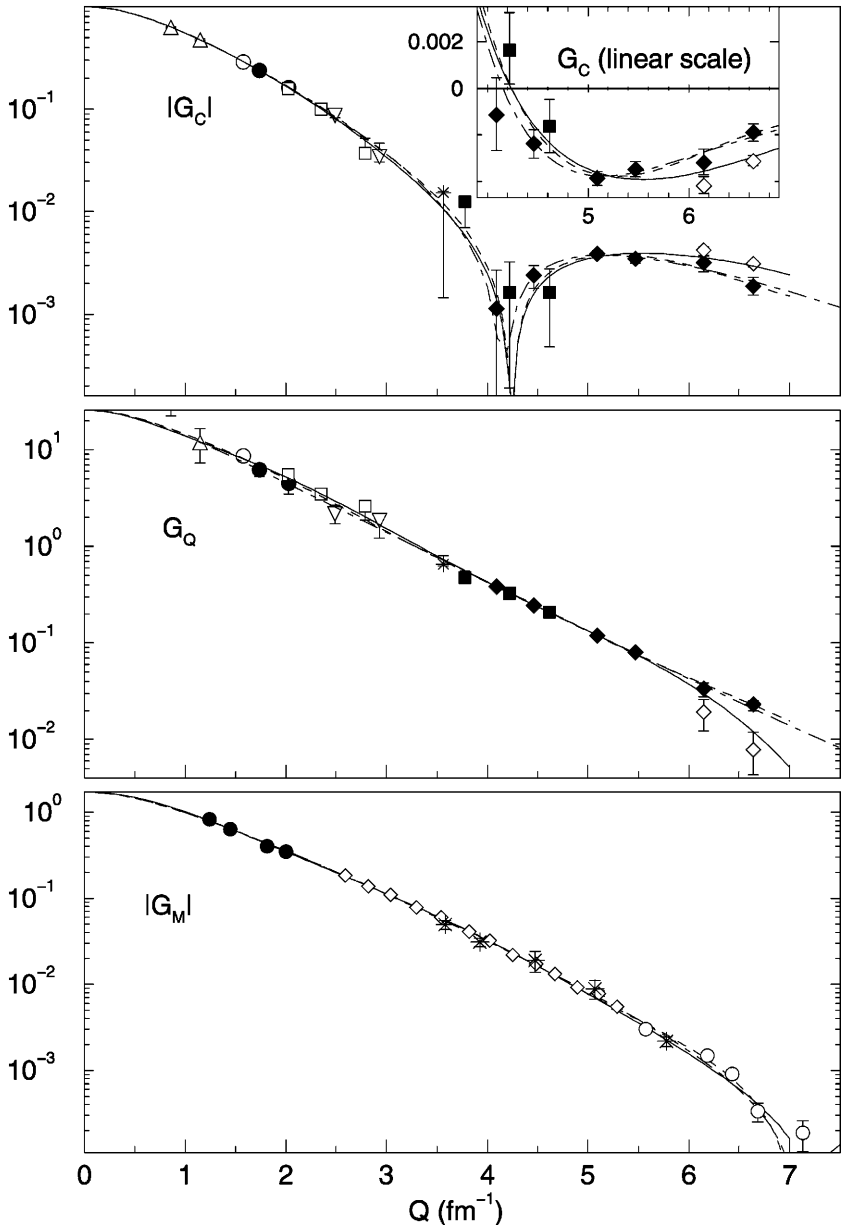

Fig. 1. Deuteron form factors G_C, G_Q and G_M as a function of Q. The data for G_C and G_Q are from Table 1, corresponding to t_{20} measurements of [21] (solid diamonds, and open diamonds for the second solution), [22] (star), [23] (open squares), [24,29] (triangles up), [25] (open circle), [26] (full squares), [27] (triangles down), [28] (full circles). The G_M data corresponds to the B measurements of [6] (open diamonds), [8] (open circles), [10] (stars), [20] (full circles). The curves are from our parameterizations I (solid line), II (dot-dashed line) and III (short dashed line)

physical limit [34]. For the sake of extracting G_C and G_Q, the interval of 68.3% confidence level $[\tilde{t}_{20} - \Delta\tilde{t}_{20}, \tilde{t}_{20} + \Delta\tilde{t}_{20}]$, and eventually the most probable value $\tilde{t}_{20}$, are then modified according to the method presented in [35]. The resulting confidence interval is entirely within the physical region ($\Delta \geq 0$). In this particular case, the modified values of p are used in (7,8) instead of the measured ones. As a result of this procedure, the errors on the form factors may be asymmetric.

The calculated values of G_C and G_Q, corresponding to all measurements of t_{20}, are presented in Table 1 and Fig. 1. The latter also shows results of parameterizations to be discussed in Sect. 3. Uncertainties come from the quoted errors in t_{20}, combined quadratically with errors on A and B reflecting the spread of the data (for example, at 5 fm^{-1}, 8.5 and 17 % respectively). For the two points of highest Q, the two solutions of (7,8) are given. The first one is preferred, based on theoretical guidance and on the parameterizations discussed below. Only parameterization I (Sect. 3.1) favors the second solution for the point at $Q = 6.64$ fm^{-1}. Note that $\tilde{t}_{20}$ need not necessarily reach its maximum allowed value, in which case the first ("+") solution would prevail from $Q = Q_{min}$ up to the undetermined node of G_Q, or to the second minimum of $\tilde{t}_{20}$, whichever occurs first.

3 Parameterization of the form factors

The three paramaterizations described below are determined through a χ^2 minimization involving 269 cross section data points [2–20] and 39 polarization data points

Table 1. Calculated values of $t_{20}(70^\circ)$, $\tilde{t}_{20}$, G_C and G_Q corresponding to all t_{20} measurements. In parantheses, statistical and systematic uncertainties are added in quadrature. For the last two points, the two solutions are given (see text)

Q (fm^{-1})	$t_{20}(70^\circ)$	$\tilde{t}_{20}$	G_C	G_Q	Ref.
0.86	-.30 (±.16)	-.30 (±.16)	.627 (±.011)	47. (±25.)	[24]
1.15	-.181 (±.070)	-.178 (±.071)	.474 (±.008)	12.0 (±4.7)	[29]
1.58	-.400 (±.037)	-.402 (±.038)	.289 (±.006)	8.66 (±.81)	[25]
1.74	-.420 (±.060)	-.423 (±.063)	.238 (±.005)	6.19 (±.90)	[28]
2.026	-.713 (±.090)	-.734 (±.095)	.160 (±.005)	5.51 (±.73)	[23]
2.03	-.590 (±.130)	-.604 (±.138)	.163 (±.005)	4.50 (±1.02)	[28]
2.352	-.896 (±.093)	-.945 (±.101)	.100 (±.004)	3.49 (±.41)	[23]
2.49	-.751 (±.153)	-.792 (±.169)	.087 (±.004)	2.17 (±.48)	[27]
2.788	-1.334 (±.233)	-1.473 (±.267)	$3.71\ (^{+1.47}_{-0.11})\times10^{-2}$	2.59 (±.073)	[23]
2.93	-1.255 (±.299)	-1.401 (±.347)	$3.45\ (^{+1.22}_{-0.39})\times10^{-2}$	$1.85\ (^{+.12}_{-.64})$	[27]
3.566	-1.87 (±1.04)	-2.20 (±1.26)	$1.53\ (^{+0.06}_{-1.38})\times10^{-2}$	$.651\ (^{+.147}_{-.023})$	[22]
3.78	-1.278 (±.186)	-1.476 (±.228)	$1.25\ (^{+.05}_{-.55})\times10^{-2}$	$.474\ (^{+.078}_{-.018})$	[26]
4.09	-.534 (±.163)	-.567 (±.193)	$-1.14\ (\pm1.6)\times10^{-3}$	.383 (±.015)	[21]
4.22	-.833 (±.153)	-.913 (±.179)	$1.63\ (^{+1.61}_{-1.44})\times10^{-3}$	.325 (±.013)	[26]
4.46	-.324 (±.089)	-.320 (±.100)	$-2.39\ (\pm.61)\times10^{-3}$	.245 (±.010)	[21]
4.62	-.411 (±.187)	-.417 (±.207)	$-1.63\ (\pm1.14)\times10^{-3}$	.208 (±.009)	[26]
5.09	.178 (±.053)	.208 ±(.056)	$-3.87\ (\pm0.30)\times10^{-3}$	.119 (±.006)	[21]
5.47	.292 (±.073)	.312 (±.075)	$-3.48\ (\pm0.32)\times10^{-3}$	.080 (±.004)	[21]
6.15	.621 (±.168)	.630 (±.170)	$-3.19\ (\pm0.55)\times10^{-3}$	$.034\ (^{+.005}_{-.006})$	
			$-4.20\ (^{+.42}_{-.32})\times10^{-3}$	.019 (±.007)	[21]
6.64	.476 (±.189)	.478 (±.189)	$-1.89\ (\pm0.38)\times10^{-3}$	$.023\ (^{+.002}_{-.003})$	
			$-3.13\ (^{+.24}_{-.19})\times10^{-3}$	.008 (±.004)	[21]

[21–29]. In most polarization data, and in some cross section data, the systematic uncertainties are dominant and may vary from point to point in a given experiment. The error considered in the χ^2 minimization is then the quadratic sum of the statistical and systematic uncertainties. The uncertainties on the parameters are given by the error matrix. For data where an overall normalization uncertainty may apply, the resulting systematic uncertainty of the fitted parameters have been evaluated by changing each individual data set by the quoted error and re-fitting the complete data set. This last procedure was carried on only with parameterization III (Sect. 3.3).

The χ^2 per degree of freedom ($\chi^2/N_{d.f.}$) all exceed the value of 1, because of systematic differences between some data sets, at the limit or beyond the quoted systematic uncertainties. Among the most recent experiments, this is the case for the A measurements of [2,4], and in a lesser extent for the t_{20} measurements of [21,26]. The fits then give an average representation of the data, though biased toward experiments with a larger number of data points.

3.1 Parameterization I

In the first parameterization (I), each form factor is given by:

$$G_X(Q^2) = G_X(0)\cdot\left[1-\left(\frac{Q}{Q_X^0}\right)^2\right]\cdot\left[1+\sum_{i=1}^{5}a_{Xi}Q^{2i}\right]^{-1}, \tag{9}$$

with $X = C, Q$ or M. This expression has the advantage of displaying explicitly the first node Q_X^0 of each form factor. The normalizing factors $G_X(0)$ are fixed by the deuteron static moments. With 18 free parameters, a fit is obtained with $\chi^2/N_{d.f.} = 1.5$.

3.2 Parameterization II

Another parameterization (II) has been proposed by Kobushkin and Syamtomov [30]. Each form factor is proportional to the square of a dipole nucleon form factor G_D and to a linear combination of reduced helicity transition amplitudes g_0, g_1, g_2:

$$\begin{pmatrix} G_C \\ G_Q \\ G_M \end{pmatrix} = G_D^2\left(\frac{Q^2}{4}\right)\cdot\mathcal{M}(\eta)\begin{pmatrix} g_0 \\ g_1 \\ g_2 \end{pmatrix}. \tag{10}$$

Each of these amplitudes is parameterized as a sum of four Lorentzian factors:

$$g_k = Q^k\sum_{i=1}^{4}\frac{a_{ki}}{\alpha_{ki}^2+Q^2}. \tag{11}$$

For each k, the α_{ki}^2 follow an arithmetical suite defined by 2 independent parameters. In addition, an asymptotic behavior dictated by quark counting rules and helicity rules valid in perturbative quantum chromodynamics (pQCD), together with the normalization conditions at $Q = 0$, imply 6 relations between the parameters a_{ki} and α_{ki} [30]. As

a result, each amplitude is described by 4 independent parameters. New parameters are obtained here, due on one hand to a newer data base, and on the other hand to the fitting of the differential cross sections instead of A and B. With 12 free parameters, a fit to the data set is obtained with $\chi^2/N_{d.f.} = 1.8$, whereas the original values of the parameters in [30] yield $\chi^2/N_{d.f.} = 7.5$. This parameterization, in contrast with the two other ones presented in this paper, can be extrapolated well above 7 fm^{-1}, albeit with some theoretical prejudice. We confirm the observation of [30,36] that the double helicity flip transition amplitude g_2 has a magnitude comparable to the zero helicity flip amplitude g_0 in the Q-range considered here, which means that these amplitudes are not in the asymptotic regime expected from pQCD.

3.3 Parameterization III

The third parameterization (III) employs a Sum-of-Gaussians (SOG) [37]. The form factors are written as

$$G_X(Q) = G_X(0) \cdot e^{-\frac{1}{4}Q^2\gamma^2} \sum_{i=1}^{25} \frac{A_i}{1+2R_i^2/\gamma^2} \cdot \left(\cos(QR_i) + \frac{2R_i^2}{\gamma^2}\frac{\sin(QR_i)}{QR_i}\right) \qquad (12)$$

Although our interest here lies in its Q-space version, the parameterization is better described in configuration space where it corresponds to a density $\rho(R)$ written as a sum of Gaussians placed at arbitrary radii R_i, with amplitudes A_i fitted to the data, and a fixed width γ. The distance R refers to the distance of the nucleons to the deuteron center of mass. The parameterization represents a totally general basis and the following applied restrictions are justified on physics grounds. First, one does not expect structures smaller than the size of the nucleon, which determines the width γ to be the size of the proton ($\gamma\sqrt{3/2} = 0.8$ fm). Second, the spacing between Gaussians is chosen slightly smaller than this width: 0.4 fm or 0.5 fm. Third, the Gaussians are placed at radii $R_i \leq R_{max} = 10$ fm, which is justified given the fact that one can easily specify the radius at which the tails of densities give no significant ($< 10^{-3}$) contribution to $G_X(Q)$. In addition, outside the range of the NN–force, the deuteron wave functions have an analytic form which is well known and depends only on the deuteron binding energy. Thus, for radii $R_i \geq 4$ fm, one can impose this shape and fix the ratio of the amplitudes A_i. Each form factor is then determined with 11 free parameters: 10 Gaussian amplitudes A_1 to A_{10}, corresponding to $R_i < 4$ fm, and one overall amplitude for the shape-given tail at $R \geq 4$ fm. With a total of 33 independent parameters, a $\chi^2/N_{d.f.}$ of 1.5 is obtained in the fit.

3.4 Results and discussion

The resulting form factors from the three parameterizations are shown in Fig. 1. As functions of two variables (Q and θ_e), the fitted quantities cannot be easily represented together with the parameterizations. In order to illustrate the quality of the fits, we present plots of relative differences of A and B, and of $\tilde{t}_{20}(Q)$ in Fig. 2. t_{21} and t_{22} are equally well fitted, which constitutes, within experimental uncertainties, an indication of the coherence of equations (1,2,3,4), and therefore of the consistency of the one-photon exchange approximation.

From the average and dispersion between the three parameterizations, combined with the fit uncertainty on Q_C^0, the node of the charge form factor is determined to be located at 4.21 ± 0.08 fm^{-1}, a value governed by the t_{20} results of [21,26]. Assuming as we do here implicitly that these two data sets have the same weight, the location of this node is not quite consistent with a relation between the two- and three-nucleon isoscalar charge form factors, established with various $N-N$ potentials [38]. The secondary maximum of $|G_C|$ is very flat, so that its location ($5.3 \pm .5$ fm^{-1}) is not determined very precisely. Its magnitude ($.0038 \pm .0003$) is clearly inconsistent with the corresponding one of the three-nucleon isoscalar charge form factor, still within the same model calculations [38]. The t_{21} results of [21], though of limited accuracy, help confirm a node of the magnetic form factor [8] at 7.2 ± 0.3 fm^{-1}. As for the first node of G_Q, according to most theoretical models, it should appear at a higher value of Q, above the range where our parameterization method applies. The value $Q_Q^0 = 7.7 \pm 0.6$ fm^{-1} given by parameterization I is probably the smallest possible value allowed by the present data. It is due to this parameterization following the downward trend of the t_{20} data point at the highest Q (see Fig. 2). This trend however is not statistically significant. Parameterization II, when extrapolated, suggests a much higher value of Q for the node of G_Q. Finally, from

$$r^2 \equiv -6\left.\frac{dG_C}{dQ^2}\right|_{Q^2=0} = 6\left[a_{C1} + (Q_C^0)^{-2}\right], \qquad (13)$$

we calculate the root mean square charge radius of the deuteron $r = 2.094 \pm 0.003$ (stat.) ± 0.009 (syst.) fm. The statistical uncertainty is given by the error matrix from parameterization I, while the systematic uncertainty is evaluated with parameterization III (see above remark about normalization uncertainties on individual data sets). This radius is 1.7% smaller than the value $r = 2.130$ fm reported in [31], consistent with expectations in the absence of corrections due to Coulomb distortion.

4 Conclusion

The extraction of the charge form factors G_C and G_Q from experiment, at given values of Q, has been reexamined. The solutions were expressed in the most compact and physical way, while a new treatment of errors was applied to polarization data at or beyond physical limits. The existing electron-deuteron elastic scattering data were used for direct parameterizations of the three deuteron electromagnetic form factors, up to

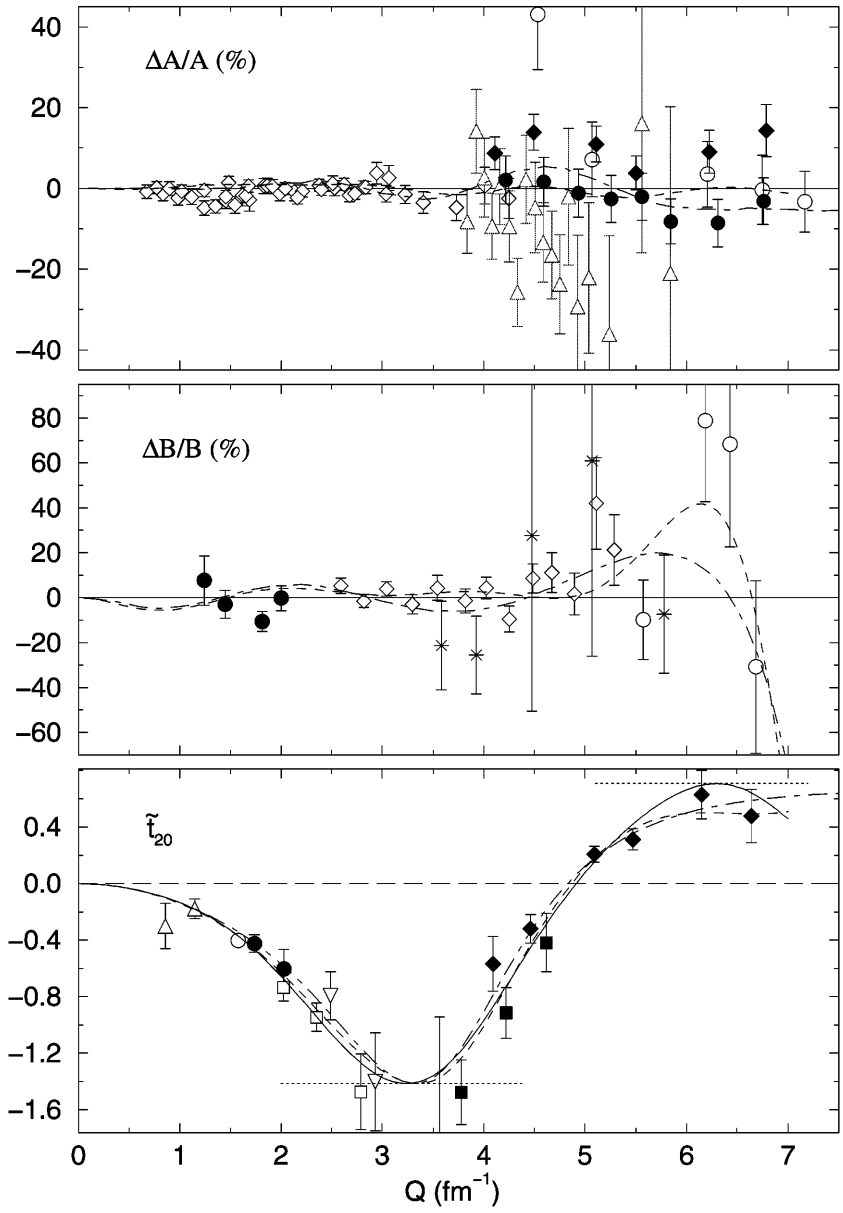

Fig. 2. (a) $\Delta A/A$, in %: deviation of A with respect to parameterization I, arbitrarily taken as a reference line; for clarity only the data from [2] (full diamonds), [4] (full circles), [5] (open circles), [12] (triangles), [18] (open diamonds) are reported. (b) $\Delta B/B$, in %. (c) $\tilde{t}_{20}$, with physical domain delimited by dotted lines. For B and $\tilde{t}_{20}$ data legend, as well as curves legend, see Fig. 1

$Q = 7$ fm^{-1}. The numerical results may be requested from the authors[1] and will be updated as new data become available in the future. The inferred value of $Q_{min} \simeq 3.3$ fm^{-1} corresponding to the minimum of $\tilde{t}_{20}$ could be used, or recalculated with such global fits, for future experiments in this Q-range [39,40], in order to resolve the discussed ambiguities in the form factors calculation. These future experiments should help confirm, or adjust, the exact value of the node of the charge form factor: this location is sensitive to the strength of the $N - N$ repulsive core, to the size of the isoscalar meson exchange contributions and to relativistic corrections. The observation of the node of the magnetic form factor [8,21] should be confirmed in a more precise experiment [41]. Together with the determination of the secondary maximum of $|G_C|$ [21], this would complete the full characterization of the deuteron electromagnetic structure up to $Q \simeq 7$ fm^{-1}.

The authors gratefully acknowledge discussions with A.P. Kobushkin and I. Sick.

This work was supported by the French Centre National de la Recherche Scientifique and Commissariat à l'Energie Atomique, the Swiss National Science Foundation, the U.S. Department of Energy and National Science Foundation, and the K.C. Wong Foundation.

[1] Contacts: jball@cea.fr (parameterizations I and II), jourdan@ubaclu.unibas.ch (III).

References

1. M.N. Rosenbluth, Phys. Rev. **79**, 615 (1950)
2. D. Abbott *et al.* (Jefferson Lab t_{20} collaboration), Phys. Rev. Lett. **82**, 1379 (1999)
3. Y.K. Akimov *et al.*, Sov. J. Phys. **29**, 335 (1979)
4. L.C. Alexa *et al.* (Jefferson Lab Hall A collaboration), Phys. Rev. Lett. **82**, 1374 (1999)
5. R.G. Arnold *et al.*, Phys. Rev. Lett. **35**, 776 (1975)
6. S. Auffret *et al.*, Phys. Rev. Lett. **54**, 649 (1985)
7. D. Benaksas *et al.*, Phys. Rev. **148**, 1327 (1966)
8. P.E. Bosted *et al.*, Phys. Rev. C **42**, 38 (1990)
9. C.D. Buchanan and R. Yearian, Phys. Rev. Lett. **15**, 303 (1965)
10. R. Cramer *et al.*, Z. Phys. **C29**, 513 (1985)
11. D.J. Drickey and L.N. Hand, Phys. Rev. Lett. **9**, 521 (1962)
12. J.E. Elias *et al.*, Phys. Rev. **9**, 521 (1969)
13. J.L. Friedman *et al.*, Phys. Rev. **120**, 992 (1960)
14. S. Galster *et al.*, Nucl. Phys. **B32**, 221 (1971)
15. D. Ganichot *et al.*, Nucl. Phys. **A178**, 545 (1972)
16. B. Grossette *et al.*, Phys. Rev. **141**, 1425 (1966)
17. F. Martin *et al.*, Phys. Rev. Lett. **38**, 1320 (1977)
18. S. Platchkov *et al.*, Nucl. Phys. **A510**, 740 (1990)
19. R.E. Rand *et al.*, Phys. Rev. Lett. **18**, 469 (1967)
20. G.G. Simon *et al.*, Nucl. Phys. **A364**, 285 (1981)
21. D. Abbott *et al.* (Jefferson Lab t_{20} collaboration), ISN-2000-01, submitted to Phys. Rev. Lett.
22. B. Boden *et al.*, Z. Phys. **C49**, 175 (1991)
23. M. Bouwhuis *et al.*, Phys. Rev. Lett. **82**, 3755 (1999)
24. V.F. Dmitriev *et al.*, Phys. Lett. **157B**, 143 (1985)
25. M. Ferro-Luzzi *et al.*, Phys. Rev. Lett. **77**, 2630 (1996)
26. M. Garçon *et al.*, Phys. Rev. C **49**, 2516 (1994)
27. R. Gilman *et al.*, Phys. Rev. Lett. **65**, 1733 (1990)
28. M.E. Schulze *et al.*, Phys. Rev. Lett. **52**, 597 (1984)
29. B.B. Voĭtsekhovskiĭ *et al.*, JETP. Lett. **43**, 733 (1986)
30. A.P. Kobushkin and A.I. Syamtomov, Phys. At. Nucl. **58**, 1477 (1995); the argument of G^2 in Eq. (7) of this paper is $Q^2/4$
31. I. Sick and D. Trautmann, Nucl. Phys. **A637**, 559 (1998)
32. S. Klarsfeld *et al.*, Nucl. Phys. **A456**, 373, (1986)
33. F.M. Lev, Sov. J. Nucl. Phys. **21**, 45 (1975), and references therein; M.P. Rekalo *et al.*, Phys. Rev. C **60**, 042202 (1999)
34. Part. Data Group, Eur. Phys. J. C **3**, 1 (1998); Sec. 29.6.6
35. G.J. Feldman and R.D. Cousins, Phys. Rev. **D57**, 3873 (1998); see Table X
36. M. Garçon *et al.* (Jefferson Lab t_{20} collaboration), Nucl. Phys. **A654**, 493c (1999)
37. I. Sick, Nucl. Phys. **A218**, 509 (1974)
38. H. Henning *et al.*, Phys. Rev. C **52**, R471 (1995)
39. W. Turchinetz *et al.*, in *Proceedings of the 2nd Workshop on Electronuclear Physics with Internal Targets and the Bates Large Acceptance Toroid, 1998*, edited by R. Alarcon and R. Milner (World Scientific, Singapore 1999), p 96
40. I. Rachek (private communication - VEPP3 experiment)
41. G.G. Petratos (private communication - JLab experiment)